

Better-Than-Chance Classification for Signal Detection

Jonathan Rosenblatt
Department of IE&M and
Zlotowsky Center for Neuroscience,
Ben Gurion University of the Negev, Israel.

Jelle Goeman
Department of Medical Statistics and Bioinformatics,
Leiden University Medical Center, The Netherlands.

Roe Gilron Roy Mukamel
Tel Aviv University, Tel Aviv University.

November 7, 2017

Abstract

We show that using a classifier’s accuracy as a test statistic, is an underpowered strategy for the purpose of finding a difference between populations, compared to a bona-fide statistical test. It is also more complicated to implement. For the cases that the purposes of the analysis is not the mere existence of a difference between populations, but rather the performance of a particular classifier, we suggest several improvements to increase power.

1 Introduction

A common workflow in neuroimaging and genetics consists of fitting a classifier, and estimating its predictive accuracy using cross validation. Given that the cross validated accuracy is a random quantity, it is then common to test if the cross validated accuracy is significantly better than chance using a permutation test. Examples in the neuroscientific literature include Golland and Fischl [2003], Pereira et al. [2009], Varoquaux et al. [2016], and especially

the recently popularized *multivariate pattern analysis* (MVPA) framework of Kriegeskorte et al. [2006]. For examples in the genetics literature see for example Golub et al. [1999], Slonim et al. [2000], Radmacher et al. [2002], Mukherjee et al. [2003], Juan and Iba [2004], Jiang et al. [2008].

To fix ideas, we will adhere to a concrete example. In Gilron et al. [2016], the authors seek to detect brain regions which encode differences between vocal and non-vocal stimuli. Following the MVPA workflow, the localization problem is cast as a supervised learning problem: if the type of the stimulus can be predicted from the brain’s activation pattern significantly better than chance, then a region is declared to encode vocal/non-vocal information. We call this an *accuracy test*, because it uses the prediction accuracy as a test statistic.

This same signal detection task can be also approached as a multivariate test. Inferring that a region encodes vocal/non-vocal information, is essentially inferring that the spatial distribution of brain activations is different given a vocal/non-vocal stimulus. As put in Pereira et al. [2009]:

... the problem of deciding whether the classifier learned to discriminate the classes can be subsumed into the more general question as to whether there is evidence that the underlying distributions of each class are equal or not.

A practitioner may thus approach the signal detection problem with a two-group location test such as Hotelling’s T^2 [Anderson, 2003]. Alternatively, if the size of the brain’s region of interest is large compared to the number of observations, so that the spatial covariance cannot be fully estimated, then a high dimensional version of Hotelling’s test can be called upon. Examples of high dimensional multivariate tests include Schäfer and Strimmer [2005], Goeman et al. [2006], or Srivastava [2007]. For brevity, and in contrast to *accuracy tests*, we will call these *location tests*, because they test for the equality of location of a multivariate distribution.

At this point, it becomes unclear which is preferable: a location test or an accuracy test? The former with a heritage dating back to Hotelling [1931], and the latter being extremely popular, as the 1,170 citations¹ of Kriegeskorte et al. [2006] suggest.

The comparison between location and accuracy tests was precisely the goal of Ramdas et al. [2016], who compared Hotelling’s T^2 location test to *Fisher’s linear discriminant analysis* (LDA) accuracy test. By comparing the rates of convergence of the power of each statistic, Ramdas et al. [2016] concluded that accuracy and location tests are rate equivalent. Rates, however, are only a first stage when comparing test statistics.

¹GoogleScholar. Accessed Aug 2017.

Asymptotic relative efficiency measures (ARE) are typically used by statisticians to compare between rate-equivalent test statistics [van der Vaart, 1998]. ARE is the limiting ratio of the samples sizes required by two statistics to achieve similar power. Ramdas et al. [2016] derive the asymptotic power functions of the two test statistics, which allows to compute the ARE between Hotelling’s T^2 (location) test and Fisher’s LDA (accuracy) test. Theorem 14.7 of van der Vaart [1998] relates asymptotic power functions to ARE. Using this theorem and the results of Ramdas et al. [2016] we deduce that the ARE is lower bounded by $2\pi \approx 6.3$. This means that Fisher’s LDA requires at least 6.3 more samples to achieve the same (asymptotic) power as the T^2 test. In this light, the accuracy test is remarkably inefficient compared to the location test. For comparison, the t-test is only 1.04 more (asymptotically) efficient than Wilcoxon’s rank-sum test [Lehmann, 2009], so that an ARE of 6.3 is strong evidence in favor of the location test.

Before discarding accuracy tests as inefficient, we recall that Ramdas et al. [2016] analyzed a *half-sample* holdout. The authors conjectured that a leave-one-out approach, which makes more efficient use of the data, may have better performance. Also, the analysis in Ramdas et al. [2016] is asymptotic. This eschews the discrete nature of the accuracy statistic, which we will show to have crucial impact. Since typical sample sizes in neuroscience are not large, we seek to study which test is to be preferred in finite samples, and not only asymptotically. Our conclusion will be quite simple: *location tests typically have more power than accuracy tests, and are easier to implement.*

Our statement rests upon the observation that with typical sample sizes, the accuracy test statistic is highly discrete. Permutation testing with discrete test statistics are known to be conservative [Hemerik and Goeman, 2014], since they are insensitive to mild perturbations of the data, and they cannot exhaust the permissible false positive rate. As put by Prof. Frank Harrell in **CrossValidated**² post back in 2011:

... your use of proportion classified correctly as your accuracy score. This is a discontinuous improper scoring rule that can be easily manipulated because it is arbitrary and insensitive.

The degree of discretization is governed by the number of samples. In our example from Gilron et al. [2016], the classification accuracy is computed using 40 examples, so that the test statistic may assume only 40 possible values. This number of examples is not unusual in a neuroimaging study.

Power loss due to discretization is further aggravated if the test statistic is highly concentrated. For an intuition consider the usage of the *resubstitution*

²A Q&A website for statistical questions: <http://stats.stackexchange.com/questions/17408/how-to-assess-statistical-significance-of-the-accuracy-of-a-classifier>

accuracy as a test statistic. This statistic simply means that the accuracy is not cross validated, but rather evaluated on the training data. If the data is high dimensional, the resubstitution accuracy will be very high due to over fitting. In a very high dimensional regime, the resubstitution accuracy will be 1 for the observed data [McLachlan, 1976, Theorem 1], but also for any permutation. The concentration of resubstitution accuracy near 1, and its discretization, render this test completely useless, with power tending to 0 for any (fixed) effect size, as the dimension of the model grows.

To compare the power of accuracy tests and location tests in finite samples, we study a battery of test statistics by means of simulation. We start with formalizing the problem in Section 2. The main findings are reported in Sections 3, and 4. A discussion follows.

2 Problem setup

2.1 Multivariate Testing

Let $y \in \mathcal{Y}$ be a class encoding. Let $x \in \mathcal{X}$ be a p dimensional feature vector. In our vocal/non-vocal example we have $\mathcal{Y} = \{0, 1\}$ and p , the number of voxels in a brain region so that $\mathcal{X} = \mathbb{R}^{27}$.

Denoting a dataset by $\mathcal{S} := \{(x_i, y_i)\}_{i=1}^n$, a multivariate test amounts to testing whether the distribution of x given $y = 1$ is the same as x given $y = 0$. I.e., we test if the multivariate voxel activation pattern has the same distribution when given a vocal stimulus, as when given a non-vocal stimulus. The comparison metric between statistics is their power, i.e., the probability to infer that $x|y = 1$ is not distributed like $x|y = 0$.

2.2 Location Tests and Hotelling's T^2

The most prevalent interpretation of “ $x|y = 1$ is not distributed like $x|y = 0$ ” is to assume they differ in means. In his seminal work, Hotelling [1931] has proposed the T^2 test statistic for testing the equality in means of two multivariate distributions. Using our notations this statistic is proportional to the difference between group means, measured with the Mahalanobis norm:

$$T^2 \propto (\bar{x}_{y=1} - \bar{x}_{y=0})' \hat{\Sigma}^{-1} (\bar{x}_{y=1} - \bar{x}_{y=0}), \quad (1)$$

where $\bar{x}_{y=j}$ is the p -vector of means in the $y = j$ group, and $\hat{\Sigma}$ is a pooled covariance estimator. Perhaps more intuitively, it can be shown that T^2 equals the Euclidean norm of the mean difference vector, after decorrelating the coordinates of x . For more background see, for example, Anderson [2003].

The major difficulty with these multivariate tests is that Σ has $p(p+1)/2$ free parameters, so that n has to be very large to apply these tests. If n is not much larger than p , or in low signal-to-noise regimes, the test is very low powered, as shown by Bai and Saranadasa [1996]. In these cases, high dimensional versions of the T^2 should be applied, which essentially regularize the estimator of Σ , thus reducing the dimensionality of the problem and improving the SNR.

2.3 Prediction Accuracy as a Test Statistic

An accuracy test amounts to setting a test statistic to be some measure prediction accuracy.

A predictor³, $\mathcal{A}_S : \mathcal{X} \rightarrow \mathcal{Y}$, is the output of a learning algorithm \mathcal{A} when applied to the dataset \mathcal{S} . The accuracy of predictor⁴, $\mathcal{E}_{\mathcal{A}_S}$, is defined as the probability of \mathcal{A}_S making a correct prediction. The accuracy of an algorithm⁵, $\mathcal{E}_{\mathcal{A}}$, is defined as the expected accuracy over all possible data sets \mathcal{S} . Formalizing, we denote by \mathcal{P} the probability measure of (x, y) , and by \mathcal{P}_S the joint probability measure of the sample \mathcal{S} . We can then write

$$\mathcal{E}_{\mathcal{A}_S} := \int_{(x,y)} \mathcal{I}\{\mathcal{A}_S(x) = y\} d\mathcal{P}(x, y), \quad (2)$$

and

$$\mathcal{E}_{\mathcal{A}} := \int_{\mathcal{S}} \mathcal{E}_{\mathcal{A}_S} d\mathcal{P}_S, \quad (3)$$

where $\mathcal{I}\{A\}$ is the indicator function⁶ of the set A .

Denoting an estimate of $\mathcal{E}_{\mathcal{A}_S}$ by $\hat{\mathcal{E}}_{\mathcal{A}_S}$, and $\mathcal{E}_{\mathcal{A}}$ by $\hat{\mathcal{E}}_{\mathcal{A}}$, a statistically significant “better than chance” estimate of either, is evidence that the classes are distinct.

Two popular estimates of $\hat{\mathcal{E}}_{\mathcal{A}}$ are the *resubstitution estimate*⁷, and the V-fold Cross Validation (CV) estimate.

Definition 1 (Resubstitution estimate). The resubstitution accuracy estimator of a learning algorithm \mathcal{A} , denoted $\hat{\mathcal{E}}_{\mathcal{A}}^{Resub}$, is defined as

$$\hat{\mathcal{E}}_{\mathcal{A}}^{Resub} := \frac{1}{n} \sum_{i=1}^n \mathcal{I}\{\mathcal{A}_S(x_i) = y_i\}. \quad (4)$$

³Known as a *hypothesis* in the machine learning literature.

⁴Known as (the complement of) the *test error* in Friedman et al. [2001]

⁵Known as (the complement of) the *expected test error* in Friedman et al. [2001]

⁶Mutatis mutandis for continuous x and y .

⁷Known as the *train error* in Friedman et al. [2001].

Definition 2 (V-fold CV estimate). Denoting by \mathcal{S}^v the v 'th partition, or *fold*, of the dataset, and by $\mathcal{S}^{(v)}$ its complement, so that $\mathcal{S}^v \cup \mathcal{S}^{(v)} = \cup_{v=1}^V \mathcal{S}^v = \mathcal{S}$, the V-fold CV accuracy estimator, denoted $\hat{\mathcal{E}}_{\mathcal{A}}^{Vfold}$, is defined as

$$\hat{\mathcal{E}}_{\mathcal{A}}^{Vfold} := \frac{1}{V} \sum_{v=1}^V \frac{1}{|\mathcal{S}^v|} \sum_{i \in \mathcal{S}^v} \mathcal{I}\{\mathcal{A}_{\mathcal{S}^{(v)}}(x_i) = y_i\}, \quad (5)$$

where $|A|$ denotes the cardinality of a set A .

2.4 How to Estimate Accuracies?

Estimating $\hat{\mathcal{E}}_{\mathcal{A}}$ requires the following design choices: Should it be resampled and how? If resampling using V-fold cross validation then How many folds? Should the data be refolded after each permutation? Should the folding be balanced?

We will now address these questions while bearing in mind that unlike the typical supervised learning setup, we are not interested in an unbiased estimate of $\mathcal{E}_{\mathcal{A}}$, but rather in the detection of its departure from chance level.

Cross validate or not? Given our goal, a biased in of $\mathcal{E}_{\mathcal{A}}$ is not a problem provided that bias is consistent over all permutations. The underlying intuition is that a permutation test will be unbiased, provided that the exact same computation is performed over all permutations. We will thus be considering both cross validated accuracies, and resubstitution accuracies.

Balanced folding? The standard practice in V-fold CV is to constrain the data folds to be balanced, i.e. stratified [e.g. Ojala and Garriga, 2010]. This means that each fold has the same number of examples from each class. We will report results with both balanced and unbalanced data foldings.

Refolding? The standard practice in neuroimaging is to permute labels and refold the data after each permutation, so that the balance of the classes in each fold is preserved. We will adhere to this practice due to its popularity, even though it is more computationally efficient to permute features instead of labels, as done by Golland et al. [2005].

How many folds? Different authors suggest different rules for the number of folds. We will look into the effect of the number of folds.

Table 1 collects an initial battery of tests we will be comparing.

Name	Algorithm	Resampling	Parameters
Hotelling	Hotelling	Resubstitution	—
Oracle	Hotelling	Resubstitution	—
Hotelling.shrink	Hotelling	Resubstitution	—
SD	Hotelling	Resubstitution	—
LDA.CV.1	LDA	V-fold	—
LDA.noCV.1	LDA	Resubstitution	—
SVM.CV.1	SVM	V-fold	cost=10
SVM.CV.2	SVM	V-fold	cost=0.1
SVM.noCV.1	SVM	Resubstitution	cost=10
SVM.noCV.2	SVM	Resubstitution	cost=0.1

Table 1: This table collects the various test statistics we will be studying. Location tests include: *Oracle*, *Hotelling*, *Hotelling.shrink*, and *SD*. *Hotelling* is the classical two-group T^2 statistic [Anderson, 2003]. *Oracle* is the same as Hotelling’s T^2 , only using the generative covariance, and not an estimated one. *Hotelling.shrink* is a high dimensional version of T^2 , with the regularized covariance from Schäfer and Strimmer [2005]. *SD* is another high dimensional version of the T^2 , from Srivastava et al. [2013]. The rest of the tests are accuracy tests, with details given in the table. For example, *SVM.CV.2* is a linear SVM, with V-fold cross validated accuracy, and cost parameter set at 0.1 [Meyer et al., 2015]. Another example is *LDA.noCV.1*, which is Fisher’s LDA, with a resubstituted accuracy estimate.

2.5 From a Test Statistic to a Permutation Test

The various test statistics in Table 1 will be compared using their power. Because our problems of interest are typically high-dimensional, i.e. $n \gg p$ does not hold, then central limit laws will not apply and we recur to permutation tests. Because we focus on two-group testing under an independent sampling assumption, we know that a label-switching permutation test is valid in that it has a false positive rate no larger than the desired level.

The sketch of our permutation test is the following: (a) Fix a test statistic. (b) Permute labels and recompute the statistic to recover its permutation distribution. (c) Declare classes differ if the observed statistic’s value is beyond its 95%’th permutation percentile.

3 Results

We now compare the power of our various statistics in various configurations. We do so via simulation, which details are now described. We start by

presenting the most basic simulation setup, and then its modifications.

3.1 Basic Simulation Setup

The following details are common to all the reported simulations, unless stated otherwise in a figure’s caption. The R code for the simulations can be found in http://www.john-ros.com/permuting_accuracy/. [TODO: populate]

Each simulation is based on 1,000 replications. In each replication, we generate n i.i.d. samples from a shift class

$$\mathbf{x}_i = \mu \mathbf{y}_i + \eta_i, \quad (6)$$

where $\mathbf{y}_i \in \mathcal{Y} = \{0, 1\}$ encodes the class of subject i , μ is a p -dimensional means vector, the noise η_i is distributed as $\mathcal{N}_p(0, \Sigma)$, the sample size $n = 40$, and the dimension of the data is $p = 23$. The covariance $\Sigma = I$. In this basic setup, reported in Figure 1, the shift effect is captured by μ . Shifts are equal in all p coordinates of μ , with coordinate-wise magnitude varying over $\{0, 1/4, 1/2\}$.

Having generated the data, we compute each of the test statistics in Table 1. For test statistics that require data folding, we used 4 folds. We then compute a permutation p-value by permuting the class labels, and recomputing each test statistic. We perform 300 such permutations. We then reject the $\mu_i = 0$ null hypothesis against a two sided alternative if the permutation p-value is smaller than 0.05. The reported power is the proportion of replication where the permutation p-value fell below 0.05.

3.2 False Positive Rate

We start with a sanity check. Theory suggests that all test statistics should control their false positive rate. Our simulations confirm this. In all our results, such as Figure 1, we encode the null case, where no signal is present and $x|y = 1$ has the same distribution as $x|y = 0$, by a red circle. Since the red circles are always below the desired 0.05 error rate (up to simulation accuracy) then the false positive rate of all test statistics, in all simulations is controlled. We may thus proceed and compare the power of each test statistic.

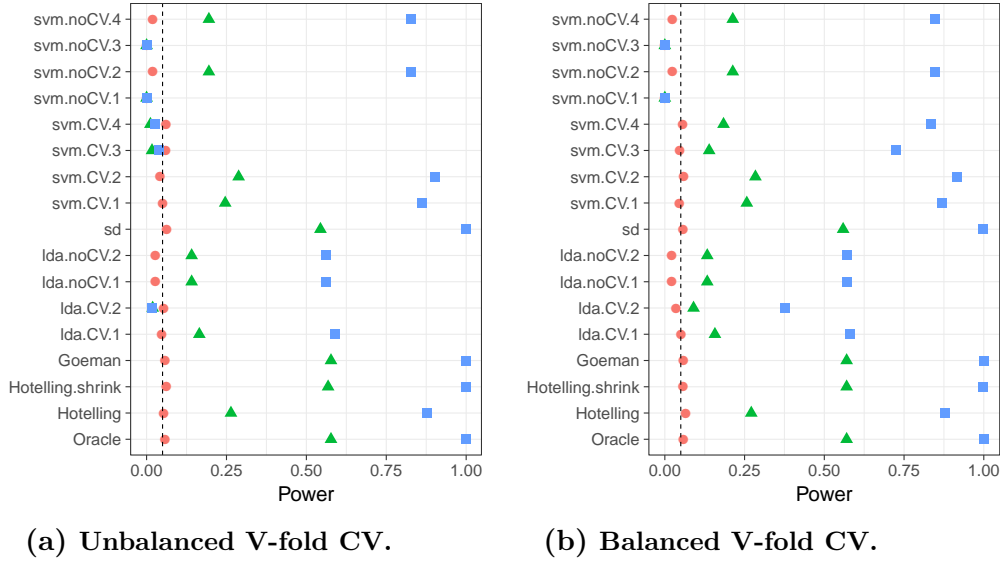
3.3 Power

Having established that all of the tests in our battery control the false positive rate, it remains to be seen if they have similar power—especially when

comparing location tests to accuracy tests.

From Figure 1 we learn that location tests are more powerful than accuracy tests. This is particularly visible for intermediate signal strength (green triangle), and location tests *SD* and *Hotelling.shrink* defined in Table 1.

Figure 1: The power of the permutation test with various test statistics. The power on the x axis. Effects are color and shape coded. The various statistics on the y axis. Their details are given in Table 1. Effects vary over $\mu = (0, \dots, 0)$ (red circle), $\mu = (0.25, \dots, 0.25)$ (green triangle), and $\mu = (0.5, \dots, 0.5)$ (blue square). Simulation details in Section 3.1. Cross-validation was performed with balanced and unbalanced data folding. See sub-captions.



3.4 Departure From Gaussianity

The Neyman-Pearson Lemma (NPL) type reasoning that favors the location test over accuracy tests may fail when the data is not multivariate Gaussian, and Hotelling's T^2 statistic no longer a generalized-likelihood-ratio test.

To check this, we replaced the multivariate Gaussian distribution of η in Eq.(6) with a heavy-tailed multivariate- t distribution. In this heavytailed setup, the dominance of the location tests was preserved, even if less evident than in the Gaussian case (Figure 2).

TODO: update figure

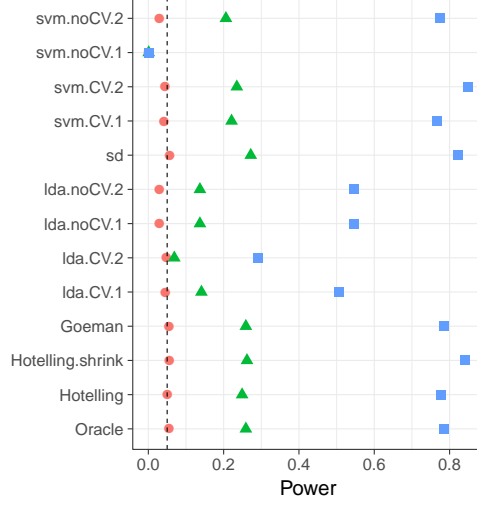


Figure 2: **Heavilytailed.** η_i is p -variate t , with $df = 3$.

3.5 Departure from Sphericity

We now test the robustness of our results to the correlations in x . In terms of Eq.(6), Σ will no longer be the identity matrix. Intuitively- both location tests and accuracy tests include the estimation of Σ , so that correlations should be accounted for. To keep the comparisons “fair” as the correlations vary, we kept the Mahalanobis norm of the signal fixed. The question remains- which test has more power: accuracy or location? We address this question using various correlation structures. We also vary the direction of the signal, μ , and distinguish between signal in the direction of the highest principal component (PC) of Σ , or the lowest.

The simulation results reveal some non trivial phenomena. First, when the signal is in the direction of the highest PC, the high dimensional location tests are far superior than accuracy tests. This holds true for the various correlation structures: the short memory correlations of $AR(1)$ in Figure 3a, the long memory correlations of a Brownian motion in Figure 4a, and the arbitrary correlation in Figure 5a.

When the signal is in the direction of the lowest PC, a different phenomenon appears. There is no clear preference between location or accuracy tests. Instead the non-regularized tests are the clear victors. This holds true for the various correlation structures: the short memory correlations of $AR(1)$ in Figure 3b, the long memory correlations of a Brownian motion in Figure 4b, and the arbitrary correlation in Figure 5b. We attribute this phenomenon to the bias introduced by the regularization, which masks the signal. This was not apparent when the signal was in the high PC, because it

had a large Euclidean norm. When the signal is in the low PC, and $\mu'\Sigma^{-1}\mu$ is fixed, then μ has a small Euclidean norm. The reader may argue that we should not have fixed $\mu'\Sigma^{-1}\mu$, thus varying μ with Σ , but rather fix the Euclidean norm of μ . This matter is discussed in Section 5.3.

Figure 3: Short memory, AR(1) correlation. $\Sigma_{k,l} = \rho^{|k-l|}$; $\rho = 0.6$

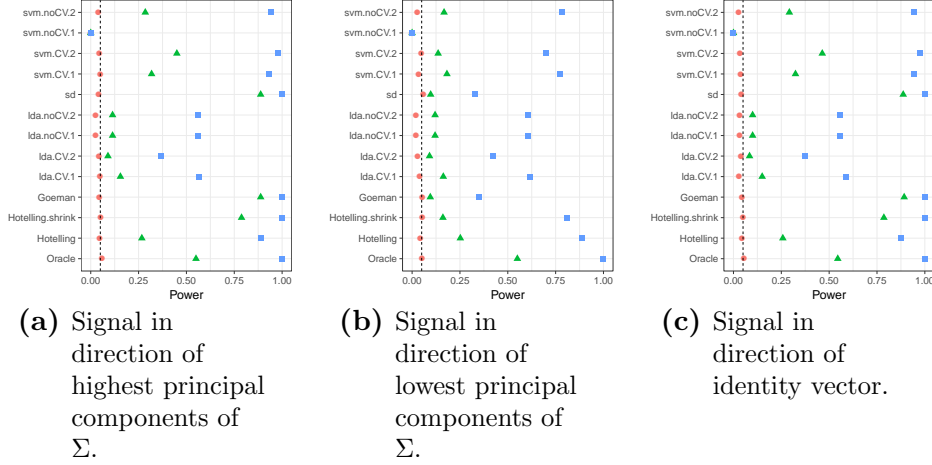
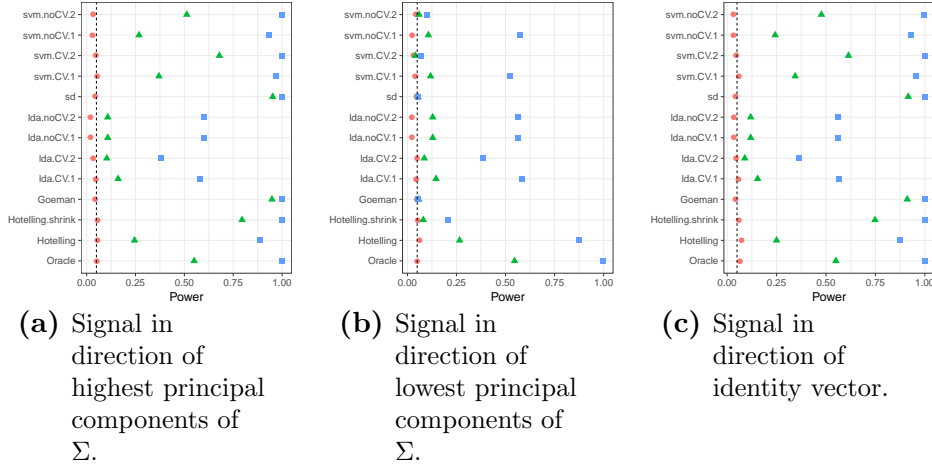
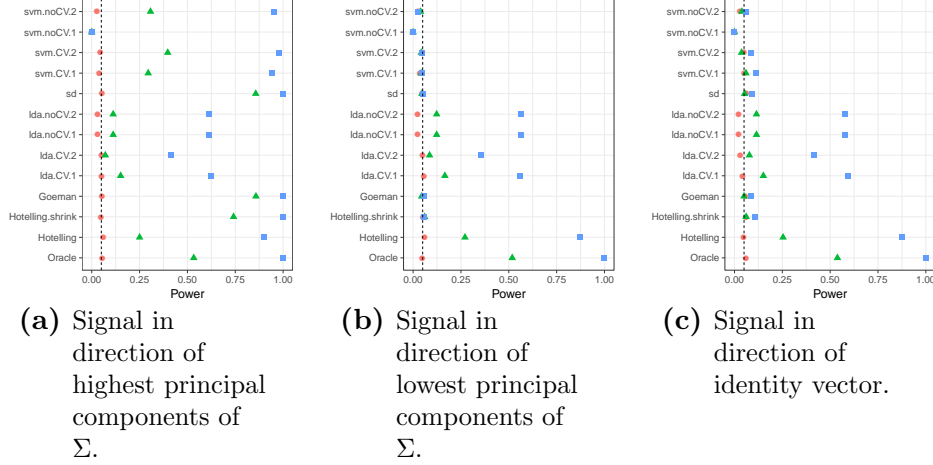


Figure 4: Long-memory Brownian motion correlation: $\Sigma = D^{-1}RD^{-1}$ where D is diagonal with $D_{jj} = \sqrt{R_{jj}}$, and $R_{k,l} = \rho \min\{k, l\}$; $\rho = 0.2$.



Our previous simulations introduce dependence between coordinates but assume all coordinates have equal variance, i.e., homoskedastic. The homoskedastic case, where difference coordinates have different variance, is of lesser importance, since we can typically normalize the variance. Some test

Figure 5: Arbitrary Correlation. $\Sigma = D^{-1}RD^{-1}$ where D is diagonal with $D_{jj} = \sqrt{R_{jj}}$, and $R = A'A$ where A is a Gaussian $p \times p$ random matrix with independent $\mathcal{N}(0, 1)$ entries.



statistics have built-in variance normalization, and are known as *affine invariant* in the statistical literature. Those that don't normalize the variance, will give less importance to noisier directions.

[TODO: update discussion.]

3.6 Departure from V-fold CV

Intuition suggests we may alleviate the discretization of the accuracy test statistic by replacing the V-fold CV, and resampling *with replacement*. The discretization of the accuracy statistic is governed by the number of examples in the union of test sets. For V-fold CV, for instance, the accuracy may assume as many values as the sample size. This suggests that the accuracy can be “smoothed” by allowing the test sample to be drawn with replacement. An algorithm that samples test sets with replacement is the *leave-one-out bootstrap estimator*, and its derivatives, such as the *0.632 bootstrap*, and *0.632+ bootstrap* [Friedman et al., 2001, Sec 7.11].

Definition 3 (bLOO). The *leave-one-out bootstrap* estimate, bLOO, is the average accuracy of the holdout observations, over all bootstrap samples. Denote by \mathcal{S}^b , a bootstrap sample b of size n , sampled with replacement from \mathcal{S} . Also denote by $C^{(i)}$ the index set of bootstrap samples not containing observation i . The leave-one-out bootstrap estimate, $\hat{\mathcal{E}}_{\mathcal{A}}^{bLOO}$, is defined as:

$$\hat{\mathcal{E}}_{\mathcal{A}}^{bLOO} := \frac{1}{n} \sum_{i=1}^n \frac{1}{|C^{(i)}|} \sum_{b \in C^{(i)}} \mathcal{I}\{\mathcal{A}_{\mathcal{S}^b}(x_i) = y_i\}. \quad (7)$$

An equivalent formulation, which stresses the Bootstrap nature of the algorithm is the following. Denoting by $S^{(b)}$ the indexes of observations that are *not* in the bootstrap sample b and are not empty,

$$\hat{\mathcal{E}}_{\mathcal{A}}^{bLOO} = \frac{1}{B} \sum_{b=1}^B \frac{1}{|S^{(b)}|} \sum_{i \in S^{(b)}} \mathcal{I}\{\mathcal{A}_{S^b}(x_i) = y_i\}. \quad (8)$$

Simulation results are reported in Figure 7 with naming conventions in Table 2. As expected, selecting test sets with replacement does increase the power of accuracy tests, when compared to V-fold cross validation, but still falls short from the power of location tests. It can also be seen that power increases with the number of bootstrap replications, since more replications reduce the level of discretization.

Name	Algorithm	Resampling	B	Parameters
LDA.Boot.1	LDA	bLOO	10	—
SVM.Boot.1	SVM	bLOO	10	cost=10
SVM.Boot.2	SVM	bLOO	10	cost=0.1
SVM.Boot.3	SVM	bLOO	50	cost=10
SVM.Boot.4	SVM	bLOO	50	cost=0.1

Table 2: The same as Table 1 for bootstrapped accuracy estimates. bLOO is defined in 3. B denotes the number of Bootstrap samples.

3.7 The Effect of High Dimension

Our setup of $n = 40$ and $p = 23$ is high dimensional in that p/n is not too small. This surfaces finite samples effects, not manifested in classical $p/n \rightarrow 0$ asymptotic analysis. Our best performing tests, *SD*, *Goeman*, and *Hottelling.shrink*, alleviate the dimensionality of the problem by regularizing the estimation of Σ , thus reducing variance at the cost of some bias. It may thus be argued that the results are driven by the regularization of the covariance, and not the test itself. The l_2 regularization in our SVM predictors, also regularize the covariance estimation, but it is certainly not the only way to regularize the covariance estimator. We thus try a shrinkage based LDA [Pang et al., 2009, Ramey et al., 2016], where *Sigma* is regularized similarly to *Hottelling.shrink*. We also try we try a diagonalized LDA⁸ [Dudoit et al., 2002], which regularizes $\hat{\Sigma}$ similarly to *SD*.

⁸Known as *Gaussian Naïve Bayes*.

Simulation results are reported in Figure 8 with naming conventions in Table 3. The proper regularization of the covariance of a classifier, just like a location test, can improve power. See, for instance, *SVM.CV.6* which is clearly better regularized than other the V-fold cross-validated accuracy tests. Compounding with a bootstrap instead of V-fold further increases the power of the test (e.g. *LDA.highdim.4*). But even so, the out-of-the-box *SD* and *Hotelling.shrink* tests have similar, if not better, performance.

Name	Algorithm	Resampling	Parameters
SVM.CV.5	SVM	V-fold	cost=100, V=4
SVM.CV.6	SVM	V-fold	cost=0.01, V=4
LDA.highdim.1	LDA	V-fold	V=4
LDA.highdim.2	LDA	V-fold	V=4
LDA.highdim.3	LDA	V-fold	V=4
LDA.highdim.4	LDA	bLOO	B=50

Table 3: The same as Table 1 for regularized (high dimensional) predictors. *SVM.CV.5* and *SVM.CV.6* are l_2 regularized SVM, with varying regularization penalty. *LDA.highdim.1* is the Diagonal Linear Discriminant Analysis of Dudoit et al. [2002]. *LDA.highdim.2* is the High-Dimensional Regularized Discriminant Analysis of Ramey et al. [2016]. *LDA.highdim.3* is the Shrinkage-based Diagonal Linear Discriminant Analysis of Pang et al. [2009]. *LDA.highdim.4* is the same with bLOO.

4 Neuroimaging Example

Figure 9 is an application of both a location and an accuracy test to the neuroimaging data of Pernet et al. [2015]. The authors of Pernet et al. [2015] collected fMRI data while subjects were exposed to the sounds of human speech (vocal), and other non-vocal sounds. Each subject was exposed to 20 sounds of each type, totaling in $n = 40$ trials. The study was rather large and consisted of about 200 subjects. The data was kindly made available by the authors at the OpenfMRI website⁹.

We perform group inference using within-subject permutations along the analysis pipeline of Stelzer et al. [2013], which was also reported in Gilron et al. [2016]. To demonstrate our point, we compare the *SD* location test with the *SVM.CV.1* accuracy test.

⁹<https://openfmri.org/>

In agreement with our simulation results, the location test (*sd*) discovers more brain regions of interest when compared to an accuracy test (*SVM.CV.1*). The former discovers 1,232 regions, while the latter only 441, as depicted in Figure 9. We emphasize that both test statistics were compared with the same permutation scheme, and the same error controls, so that any difference in detections is due to their different power.

5 Discussion

We have set out to understand which of the tests is more powerful: accuracy tests or location tests. Our practical advice for the practitioner, is that accuracy tests are never optimal. There is always a multivariate test, possibly a location test, that dominates in power. The class of location tests we examined, in particular their regularized versions, are good performers in a wide range of simulation setups and empirically. They are also typically easier to implement, and faster to run, since no cross validation will be involved. Their high-dimensional versions, such as Schäfer and Strimmer [2005], Goeman et al. [2006], and Srivastava [2007], are particularly well suited for empirical problems such as neuroimaging and genetics.

5.1 Where do Accuracy Tests Lose Power?

The low power of the accuracy tests compared to location tests can be attributed to the following causes:

(a) **Discretization:** The discrete nature of accuracy test statistics. The degree of discretization is governed by the sample size. For this reason, an asymptotic analysis such as Ramdas et al. [2016], or Golland et al. [2005], will not capture power loss due to discretization¹⁰. This type of analysis render resubstitution accuracy estimates a legitimate asymptotic test, while they are a terrible finite sample test.

(b) **Shift Alternatives:** We focused on shift alternatives, so a NPL type argument will naturally favor location tests. On the other hand: (i) Our empirical results in Section 4 also favors location tests. (ii) Location tests can also be preferable when departing from shift alternative such as in scale alternatives (Fig. ??) and mixture alternatives (Fig. 9). (iii) We have never observed a case where an accuracy test had considerable more power than a location test. The discretization argument alone suffice to state that there will always be a test statistic with more power than an accuracy test.

¹⁰This actually holds for all power analyses relying on a *contiguity* argument [van der Vaart, 1998, Ch.6].

- (c) **Inefficient** use of the data when validating with a holdout set.
- (d) Inappropriate **regularization** in high SNR regimes: testing requires less regularization than predicting.

TODO: add $n=400$ to isolate NPL versus discretization with 1,000 replications

5.2 Interpretation

Multivariate tests, and location tests in particular, are easier to interpret. To do so we typically use a NPL type argument, and think of the type of signal a test is sensitive to. Accuracy tests are seen as “black boxes”, even though they can be analyzed in the same way. Gilron et al. [2017] demonstrate that the type of signal captured by accuracy tests is less interpretable to neuroimaging practitioners than location tests.

5.3 Fixed SNR

For a fair comparisons between simulations, in particular between those with different correlations, we needed to fix the difficulty of the problem. We defined “a fair comparison” to be such that a maximal power test would have the same power, justifying our choice of fixing the Mahalanobis norm of μ . Formally, in all our simulations we set $\mu\Sigma^{-1}\mu = p$.

Our choice implies that the Euclidean norm of μ varies with the covariance, and with the direction of the signal, so that detecting signal in the low PCs is not easier than detecting signal in the high PCs. Quantitatively, fixing the Mahalanobis norm implies that the Euclidean norm of μ is proportional to the eigenvalue of the corresponding eigenvector: μ will have a large Euclidean norm in the high PCs and small Euclidean norm in the low PCs.

[TODO: add simulation with fixed Euclidean norm]

5.4 High Versus Low PCs

TODO. In particular bias in low PCs.

5.5 Testing in Augmented Spaces

It may be argued that only accuracy tests permits the separation between classes in high dimensions, such as in *reproducing kernel Hilbert spaces* (RKHS) by using non-linear predictors. This is a false argument— accuracy tests do not have any more flexibility than location tests. Indeed, it is possible to

test for location in the same space the classifier is learned. For independence tests in high dimensional spaces see for example Székely and Rizzo [2009] or Gretton et al. [2012].

5.6 A Good Accuracy Test

Brain-computer interfaces and clinical diagnostics [e.g. Olivetti et al., 2012, Wager et al., 2013] are examples where we want to know not only if information is encoded in a region, but rather, that a particular predictor can extract it. In these cases an accuracy test cannot be replaced by a location, or other, statistical test. For these cases, we collect some conclusions and best practices.

Sample size. The conservativeness of accuracy tests decrease with sample size.

Regularize. Regularization proves crucial to detection power in low SNR regimes, which may be due to strong correlations or high-dimension. We find that the Shrinkage-based Diagonal Linear Discriminant Analysis of Pang et al. [2009] is a particularly good performer, but more research is required on this matter.

Smooth accuracy. Smooth accuracy estimate by cross validating with replacement. The bLOO estimator, in particular, is preferable over V-fold.

Permute features. Permuting features, instead of labels, is computationally more efficient than permuting labels, because refolding can be done once, for all permutations. It allows to preserve the balance of folds after a permutation, without refolding.

Resubstitution accuracy in high SNR. Resubstitution accuracy is useful in high SNR regimes, such as $n \gg p$, because it avoids cross validation without compromising power. In low SNR, the power loss is considerable. We attribute this to the compounding of discretization and concentration effects: the difference between the sampling distribution of the resubstitution accuracy is simply indistinguishable under the null and under the alternative. In high SNR, the concentration is less impactful, and the computational burden of cross validation can be avoided by using the resubstitution accuracy.

5.7 Related Literature

Ojala and Garriga [2010] study the power of two accuracy tests differing in their permutation scheme: One testing the “no signal” null hypothesis, and the other testing the “independent features” null hypothesis. They perform an asymptotic analysis, and a simulation study. They also apply various classifiers to various data sets. Their emphasis is the effect of the underlying classifier on the power, and the potential of the “independent features” test for feature selection. This is a very different emphasis from our own.

Olivetti et al. [2012] and Olivetti et al. [2014] looked into the problem of choosing a good accuracy test. They propose a new test they call an *independence test*, and demonstrate by simulation that it has more power than other accuracy tests, and can deal with non-balanced data sets. We did not include this test in the battery we compared, but we note that the independence test of Olivetti et al. [2012] relies on a discrete test statistic. It may thus be improved by regularizing and resampling with replacement, before the application of Olivetti et al. [2012]’s test statistic.

Golland and Fischl [2003] and Golland et al. [2005] study accuracy tests using simulation, neuroimaging data, genetic data, and analytically. Their analytic results formalize our intuition from Section 1 on the effect of concentration of the accuracy statistic: The finite Vapnik–Chervonenkis dimension requirement [Golland et al., 2005, Sec 4.3] prevents the permutation p-value from (asymptotically) concentrating near 1. Like us, they find that the power increases with the size of the test set. This is seen in Fig.4 of Golland et al. [2005], where the size of the test-set, K , governs the discretization. Since they permute features, not labels, then all their permutation samples are balanced, and there is no issue of refolding.

Golland et al. [2005] simulate the power of accuracy tests by sampling from a Gaussian mixture family of models, and not from a location family as our own simulations. Under their model (with some abuse of notation)

$$\begin{aligned}(x_i|y_i = 1) &\sim \pi\mathcal{N}(\mu_1, I) + (1 - \pi)\mathcal{N}(\mu_2, I), \\ (x_i|y_i = 0) &\sim (1 - \pi)\mathcal{N}(\mu_1, I) + \pi\mathcal{N}(\mu_2, I).\end{aligned}$$

Varying π interpolates between the null distribution ($\pi = 0.5$) and a location shift model ($\pi = 0$). We now perform the same simulation as Golland et al. [2005], and in the same dimensionality as our previous simulations. We re-parameterize so that $\pi = 0$ corresponds to the null model:

$$\begin{aligned}(x_i|y_i = 1) &\sim (1/2 - \pi)\mathcal{N}(\mu_1, I) + (1/2 + \pi)\mathcal{N}(\mu_2, I), \\ (x_i|y_i = 0) &\sim (1/2 + \pi)\mathcal{N}(\mu_1, I) + (1/2 - \pi)\mathcal{N}(\mu_2, I).\end{aligned}\tag{9}$$

Rosenblatt and Benjamini [2017] show that a location test may be suboptimal for mixture alternatives, but when compared to Wilcoxon’s signed rank test, and not to an accuracy tests. From our results, reported in Figure 10, we see that for the mixture class of Golland et al. [2005] locations tests are to be preferred.

5.8 Epilogue

Given all the above, we find the popularity of accuracy tests for signal detection quite puzzling. We believe this is due to a reversal of the inference cascade. Researchers first fit a classifier, and then ask if the classes are any different. Were they to start by asking if classes are any different, and only then try to classify, then location tests would naturally arise as the preferred method. As put by Ramdas et al. [2016]:

The recent popularity of machine learning has resulted in the extensive teaching and use of prediction in theoretical and applied communities and the relative lack of awareness or popularity of the topic of Neyman-Pearson style hypothesis testing in the computer science and related “data science” communities.

6 Acknowledgments

JDR was supported by the ISF 900/60 research grant. JDR also wishes to Yuval Benjamini, Jesse B.A. Hemerik, Yakir Brechenko, Omer Shamir, Joshua Vogelstein, Gilles Blanchard, and Jason Stein for their valuable inputs.

References

- T. W. Anderson. *An Introduction to Multivariate Statistical Analysis*. Wiley-Interscience, Hoboken, NJ, 3 edition edition, July 2003. ISBN 978-0-471-36091-9.
- Z. Bai and H. Saranadasa. Effect of high dimension: by an example of a two sample problem. *Statistica Sinica*, pages 311–329, 1996.
- Y. Benjamini and Y. Hochberg. Controlling the false discovery rate: a practical and powerful approach to multiple testing. *JOURNAL-ROYAL STATISTICAL SOCIETY SERIES B*, 57:289–289, 1995.
- S. Dudoit, J. Fridlyand, and T. P. Speed. Comparison of Discrimination Methods for the Classification of Tumors Using Gene Expression Data. *Journal of the American Statistical Association*, 97(457):77–87, Mar. 2002. ISSN 0162-1459. doi: 10.1198/016214502753479248.
- J. Friedman, T. Hastie, and R. Tibshirani. *The elements of statistical learning*, volume 1. Springer series in statistics New York, 2001.
- J. Friedman, T. Hastie, and R. Tibshirani. Regularization Paths for Generalized Linear Models via Coordinate Descent. *Journal of Statistical Software*, 33(1):1–22, 2010.
- R. Gilron, J. Rosenblatt, O. Koyejo, R. A. Poldrack, and R. Mukamel. Quantifying spatial pattern similarity in multivariate analysis using functional anisotropy. *arXiv:1605.03482 [q-bio]*, May 2016.
- R. Gilron, J. Rosenblatt, O. Koyejo, R. A. Poldrack, and R. Mukamel. What’s in a pattern? examining the type of signal multivariate analysis uncovers at the group level. *NeuroImage*, 146:113–120, 2017.
- J. J. Goeman, S. A. Van De Geer, and H. C. Van Houwelingen. Testing against a high dimensional alternative. *Journal of the Royal Statistical Society: Series B (Statistical Methodology)*, 68(3):477–493, 2006.
- P. Golland and B. Fischl. Permutation tests for classification: towards statistical significance in image-based studies. In *IPMI*, volume 3, pages 330–341. Springer, 2003.
- P. Golland, F. Liang, S. Mukherjee, and D. Panchenko. Permutation Tests for Classification. In P. Auer and R. Meir, editors, *Learning Theory*, number 3559 in Lecture Notes in Computer Science, pages 501–515. Springer Berlin

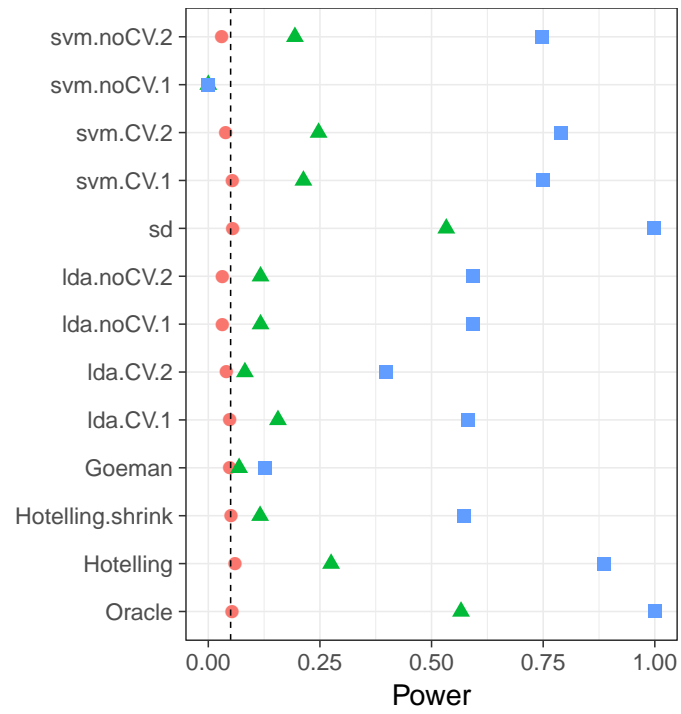
- Heidelberg, June 2005. ISBN 978-3-540-26556-6 978-3-540-31892-7. doi: 10.1007/11503415_34.
- T. R. Golub, D. K. Slonim, P. Tamayo, C. Huard, M. Gaasenbeek, J. P. Mesirov, H. Coller, M. L. Loh, J. R. Downing, M. A. Caligiuri, C. D. Bloomfield, and E. S. Lander. Molecular Classification of Cancer: Class Discovery and Class Prediction by Gene Expression Monitoring. *Science*, 286(5439):531–537, Oct. 1999. ISSN 0036-8075, 1095-9203. doi: 10.1126/science.286.5439.531.
- A. Gretton, K. M. Borgwardt, M. J. Rasch, B. Schölkopf, and A. Smola. A Kernel Two-sample Test. *J. Mach. Learn. Res.*, 13:723–773, Mar. 2012. ISSN 1532-4435.
- J. Hemerik and J. Goeman. Exact testing with random permutations. *arXiv:1411.7565 [math, stat]*, Nov. 2014.
- H. Hotelling. The Generalization of Student’s Ratio. *The Annals of Mathematical Statistics*, 2(3):360–378, Aug. 1931. ISSN 0003-4851, 2168-8990. doi: 10.1214/aoms/1177732979.
- W. Jiang, S. Varma, and R. Simon. Calculating confidence intervals for prediction error in microarray classification using resampling. *Statistical Applications in Genetics and Molecular Biology*, 7(1), 2008.
- L. Juan and H. Iba. Prediction of tumor outcome based on gene expression data. *Wuhan University Journal of Natural Sciences*, 9(2):177–182, Mar. 2004. ISSN 1007-1202, 1993-4998. doi: 10.1007/BF02830598.
- N. Kriegeskorte, R. Goebel, and P. Bandettini. Information-based functional brain mapping. *Proceedings of the National Academy of Sciences of the United States of America*, 103(10):3863–3868, July 2006. ISSN 0027-8424, 1091-6490. doi: 10.1073/pnas.0600244103.
- E. L. Lehmann. Parametric versus nonparametrics: two alternative methodologies. *Journal of Nonparametric Statistics*, 21(4):397–405, 2009. ISSN 1048-5252. doi: 10.1080/10485250902842727.
- C. Ley, D. Paindaveine, and T. Verdebout. High-dimensional tests for spherical location and spiked covariance. *Journal of Multivariate Analysis*, 139: 79–91, 2015.
- G. J. McLachlan. The bias of the apparent error rate in discriminant analysis. *Biometrika*, 63(2):239–244, Jan. 1976. ISSN 0006-3444, 1464-3510. doi: 10.1093/biomet/63.2.239.

- D. Meyer, E. Dimitriadou, K. Hornik, A. Weingessel, and F. Leisch. *e1071: Misc Functions of the Department of Statistics, Probability Theory Group (Formerly: E1071), TU Wien*. 2015. R package version 1.6-7.
- S. Mukherjee, P. Tamayo, S. Rogers, R. Rifkin, A. Engle, C. Campbell, T. R. Golub, and J. P. Mesirov. Estimating dataset size requirements for classifying DNA microarray data. *Journal of Computational Biology: A Journal of Computational Molecular Cell Biology*, 10(2):119–142, 2003. ISSN 1066-5277. doi: 10.1089/106652703321825928.
- M. Ojala and G. C. Garriga. Permutation Tests for Studying Classifier Performance. *Journal of Machine Learning Research*, 11(Jun):1833–1863, 2010. ISSN 1533-7928.
- E. Olivetti, S. Greiner, and P. Avesani. Induction in Neuroscience with Classification: Issues and Solutions. In G. Langs, I. Rish, M. Grosse-Wentrup, and B. Murphy, editors, *Machine Learning and Interpretation in Neuroimaging*, number 7263 in Lecture Notes in Computer Science, pages 42–50. Springer Berlin Heidelberg, 2012. ISBN 978-3-642-34712-2 978-3-642-34713-9. doi: 10.1007/978-3-642-34713-9_6.
- E. Olivetti, S. Greiner, and P. Avesani. Statistical independence for the evaluation of classifier-based diagnosis. *Brain Informatics*, 2(1):13–19, Dec. 2014. ISSN 2198-4018, 2198-4026. doi: 10.1007/s40708-014-0007-6.
- H. Pang, T. Tong, and H. Zhao. Shrinkage-based Diagonal Discriminant Analysis and Its Applications in High-Dimensional Data. *Biometrics*, 65(4):1021–1029, Dec. 2009. ISSN 1541-0420. doi: 10.1111/j.1541-0420.2009.01200.x.
- F. Pereira, T. Mitchell, and M. Botvinick. Machine learning classifiers and fMRI: A tutorial overview. *NeuroImage*, 45(1, Supplement 1):S199–S209, Mar. 2009. ISSN 1053-8119. doi: 10.1016/j.neuroimage.2008.11.007.
- C. R. Pernet, P. McAleer, M. Latinus, K. J. Gorgolewski, I. Charest, P. E. G. Bestelmeyer, R. H. Watson, D. Fleming, F. Crabbe, M. Valdes-Sosa, and P. Belin. The human voice areas: Spatial organization and inter-individual variability in temporal and extra-temporal cortices. *NeuroImage*, 119:164–174, Oct. 2015. ISSN 1053-8119. doi: 10.1016/j.neuroimage.2015.06.050.
- M. D. Radmacher, L. M. McShane, and R. Simon. A Paradigm for Class Prediction Using Gene Expression Profiles. *Journal of Computational Biology*, 9(3):505–511, June 2002. ISSN 1066-5277. doi: 10.1089/106652702760138592.

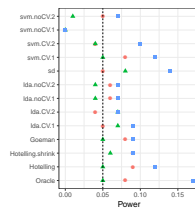
- A. Ramdas, A. Singh, and L. Wasserman. Classification Accuracy as a Proxy for Two Sample Testing. *arXiv:1602.02210 [cs, math, stat]*, Feb. 2016.
- J. A. Ramey, C. K. Stein, P. D. Young, and D. M. Young. High-Dimensional Regularized Discriminant Analysis. *arXiv preprint arXiv:1602.01182*, 2016.
- J. D. Rosenblatt and Y. Benjamini. On mixture alternatives and wilcoxon’s signed-rank test. *The American Statistician*, (just-accepted), 2017.
- J. Schäfer and K. Strimmer. A Shrinkage Approach to Large-Scale Covariance Matrix Estimation and Implications for Functional Genomics. *Statistical Applications in Genetics and Molecular Biology*, 4(1), Jan. 2005. ISSN 1544-6115. doi: 10.2202/1544-6115.1175.
- D. K. Slonim, P. Tamayo, J. P. Mesirov, T. R. Golub, and E. S. Lander. Class Prediction and Discovery Using Gene Expression Data. In *Proceedings of the Fourth Annual International Conference on Computational Molecular Biology*, RECOMB ’00, pages 263–272, New York, NY, USA, 2000. ACM. ISBN 978-1-58113-186-4. doi: 10.1145/332306.332564.
- M. S. Srivastava. Multivariate Theory for Analyzing High Dimensional Data. *Journal of the Japan Statistical Society*, 37(1):53–86, 2007. doi: 10.14490/jjss.37.53.
- M. S. Srivastava, S. Katayama, and Y. Kano. A two sample test in high dimensional data. *Journal of Multivariate Analysis*, 114:349–358, Feb. 2013. ISSN 0047-259X. doi: 10.1016/j.jmva.2012.08.014.
- J. Stelzer, Y. Chen, and R. Turner. Statistical inference and multiple testing correction in classification-based multi-voxel pattern analysis (MVPA): Random permutations and cluster size control. *NeuroImage*, 65:69–82, Jan. 2013. ISSN 1053-8119. doi: 10.1016/j.neuroimage.2012.09.063.
- G. J. Székely and M. L. Rizzo. Brownian distance covariance. *The Annals of Applied Statistics*, 3(4):1236–1265, Dec. 2009. ISSN 1932-6157, 1941-7330. doi: 10.1214/09-AOAS312.
- A. W. van der Vaart. *Asymptotic Statistics*. Cambridge University Press, Cambridge, UK ; New York, NY, USA, Oct. 1998. ISBN 978-0-521-49603-2.
- G. Varoquaux, P. R. Raamana, D. Engemann, A. Hoyos-Idrobo, Y. Schwartz, and B. Thirion. Assessing and tuning brain decoders: cross-validation, caveats, and guidelines. working paper or preprint, June 2016.

T. D. Wager, L. Y. Atlas, M. A. Lindquist, M. Roy, C.-W. Woo, and E. Kross.
An fMRI-Based Neurologic Signature of Physical Pain. *New England Journal of Medicine*, 368(15):1388–1397, Apr. 2013. ISSN 0028-4793. doi:
10.1056/NEJMoa1204471.

Figure 6: Heteroskedasticity: Σ is diagonal with $\Sigma_{jj} = j$.



(a) TODO: caption.



(b) TODO: figure.

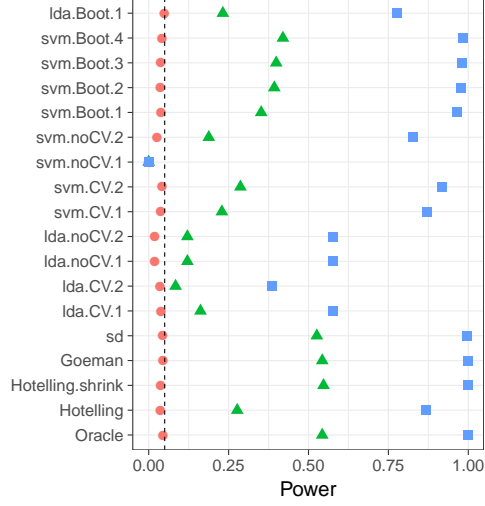


*Figure 7: **Bootstrap.*** The power of a permutation test with various test statistics. The power on the x axis. Effects are color and shape coded. The various statistics on the y axis. Their details are given in tables 1 and 2. Effects vary over 0 (red circle), 0.25 (green triangle), and 0.5 (blue square). Simulation details in Appendix 3.1.

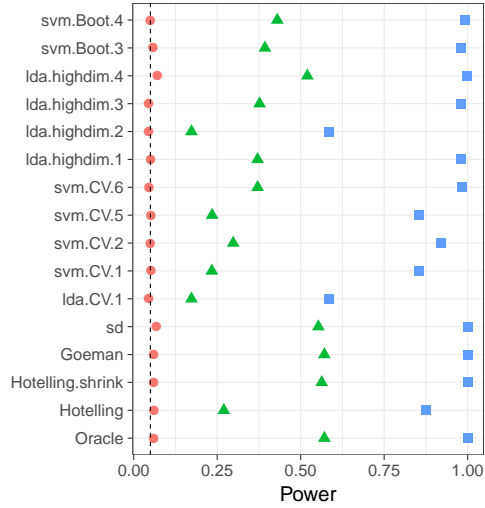


*Figure 8: **HighDim Classifier.*** The power of a permutation test with various test statistics. The power on the x axis. Effects are color and shape coded. The various statistics on the y axis. Their details are given in tables 1 and 3. Effects vary over 0 (red circle), 0.25 (green triangle), and 0.5 (blue square). Simulation details in Section 3.1.

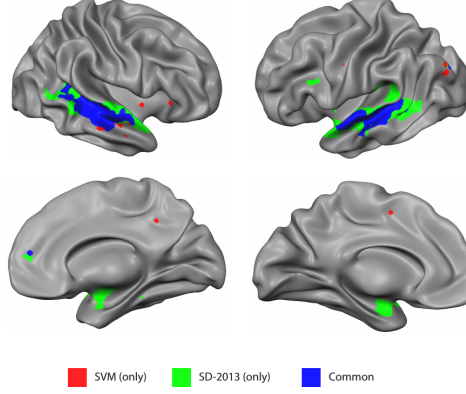


Figure 9: Brain regions encoding information discriminating between vocal and non-vocal stimuli. Map reports the centers of 27-voxel sized spherical regions, as discovered by an accuracy test (*SVM.CV.1*), and a location test (*SD*). *SVM.CV.1* was computed using 5-fold cross validation, and a cost parameter of 1. Region-wise significance was determined using the permutation scheme of Stelzer et al. [2013], followed by region-wise $FDR \leq 0.05$ control using the Benjamini-Hochberg procedure [Benjamini and Hochberg, 1995]. Number of permutations equals 400. The location test detect 1,232 regions, and the accuracy test 441, 399 of which are common to both. For the details of the analysis see Gilron et al. [2016].

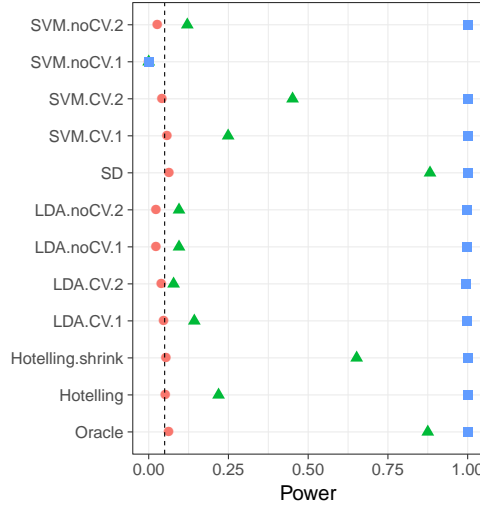


Figure 10: Mixture Alternatives. \mathbf{x}_i is distributed as in Eq.(9). μ is a p -vector with $3/\sqrt{p}$ in all coordinates. The effect, π , is color and shape coded and varies over 0 (red circle), $1/4$ (green triangle) and $1/2$ (blue square).